

Development of a Wave Absorbing System Using a Liquefied Sandbed

YOON-KOO KANG* AND SHIGEO TAKAHASHI**

*Port Management Team, Engineering & Construction Group, Samsung Corporation, Sunghnam, Gyonggi, Korea
**Port and Airport Research Institute, Yokosuka, Japan

KEY WORDS: Liquefied sandbed, Wave absorbing system, Wave damping, Water supply pipes, Wave-induced sandbed compaction

ABSTRACT: A new wave-absorbing system, called the liquefied sandbed wave barrier (LSWB) system, is currently under development at the Port and Airport Research Institute (PARI) of Japan. The wave damping effect by the LSBW system is substantial, as confirmed by small-scale experiments and FEM numerical calculations, i.e., the wave transmission coefficient of the system is less than 0.2. Here, the results of large-scale experiments are discussed in view of practical application. Although the LSBW system provides high wave damping, nearly equal to theoretical values, difficulty exists in obtaining a homogeneously liquefied sandbed, due to the occurrence of liquefied sandbed compaction by cyclic wave loading, which in turn, reduces excess pore pressure and the wave damping effect. These two phenomena primarily occur when the sandbed is composed of fine sand with small permeability. Based on experimental results, we propose a design method that includes countermeasures against such problems, and a prototype LSBW system is constructed in a very large wave flume at PARI. Wave damping by the prototype LSBW system is confirmed to be quite stable and high, as predicted by theoretical calculations.

1. Introduction

1.1 Concept of LSBW system

To dissipate wave energy using damping produced by the movement of liquefied sand, we have been developing a liquefied sandbed wave barrier (LSWB) system consisting of horizontal pipes buried in the sandbed (Fig. 1), being a unique wave barrier in that it requires no structure. By pumping water through the pipes, the pore pressure in the sand bed is increased and "sand liquefaction (boiling)" occurs; an effect which significantly decreases the shear modulus of the sandbed such that large movement of the sand occurs due to wave action. This causes wave energy dissipation by friction among the sand particles during their wave-induced movement.

While it is generally known that waves traveling on a seabed are damped due to surface friction and inner percolation (Gade, 1958; Putnam and Johnson, 1949; Reid and Kajiura, 1957), they are also damped by movement of the seabed itself. For example, Yamamoto and Takahashi (1985) theoretically and experimentally studied wave-seabed interactions and found that wave damping due to the movement of soft clay is large. With regard to sand, however, they concluded that wave damping by sand movement is much less due to its high shear modulus.

1.2 Development of LSBW system

When a seabed is sufficiently soft, it can produce very large wave damping similar to that produced by soft clay. We have determined that a "very soft sandbed" can be created by liquefying the sandbed using pore water supplied from the bottom of the sandbed. A series of studies aimed at developing a LSBW system has been carried out at PARI since 1992. Figure 2 shows a photograph of typical wave damping during a small-scale experiment in which the liquefied sandbed is 40 cm thick and 4 m long. Regular waves with a 1 s wave period and 8-cm wave height are generated in 25 cm deep water. As shown, wave heights are substantially decreased by passing over a liquefied sandbed, i.e., wave height at the onshore side is reduced by more than 75 %. This series of model experiments confirmed the wave damping effect of the LSBW system (Takahashi et al., 1994).

Assuming a homogeneously liquefied sandbed, a FEM numerical calculation method was developed in the linear

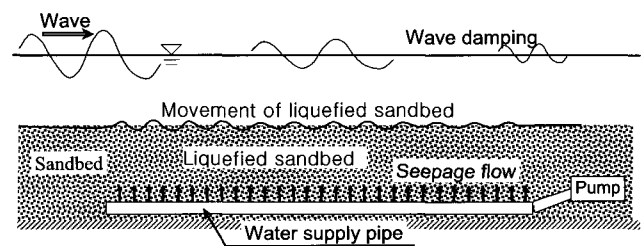


Fig. 1 Schematic diagram of LSBW for a wave energy absorbing system

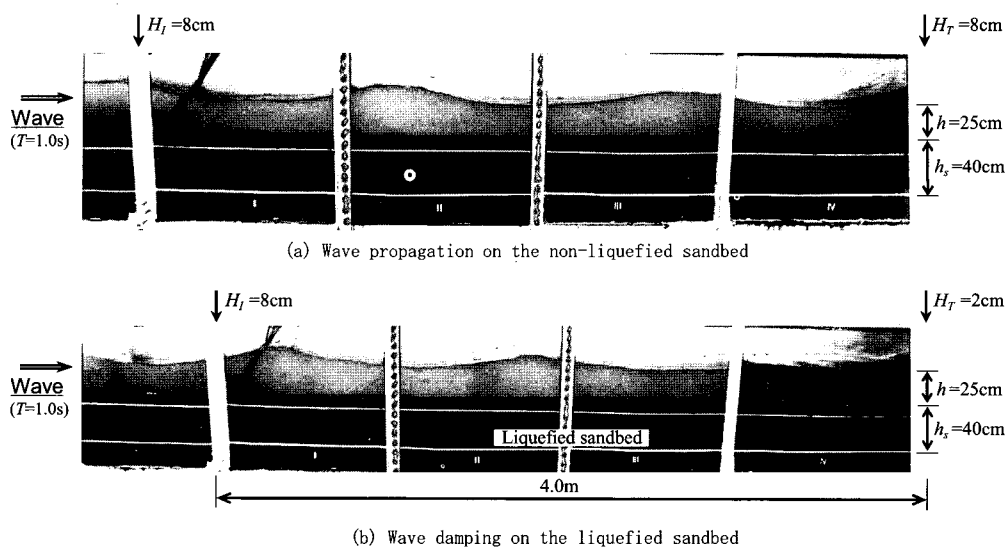


Fig. 2 Wave damping by a liquefied sandbed in a small wave flume

frequency domain using Biot's two-phase theory (Biot, 1962) and Yamamoto's wave damping theory (Yamamoto and Takahashi, 1985), with theoretical calculations well expressing wave damping. For example, the wave transmission coefficient can be 0.2-0.4 through a LSWB system having a length equal to one wavelength and sandbed thickness equal to the water depth.

1.3 Critical problems and study objective

Here, we describe a series of large-scale model experiments designed to investigate in detail LSWB characteristics for practical-use application. Experiments are conducted in a large wave flume with two kinds of sandbed. Results indicate two critical problems:

- (1) difficulty exists in obtaining a homogeneously liquefied sandbed, and
- (2) compaction of the liquefied sandbed occurs by cyclic wave loading such that excess pore pressure and the wave-damping effect are reduced.

Both these phenomena are particularly apparent when the sandbed is made of the fine sand with small permeability; conditions which are needed to reduce water-supply electric power requirements in comparison with using coarse sand.

Accordingly, here we use experiments to elucidate these critical problems, describing and discussing noteworthy interactions between waves and the liquefied sandbed. In addition, a LSWB prototype system designed using experimental results was constructed in a very large wave flume recently installed at PARI, with subsequent results obtained from prototype experiments being presented here as well.

2. Large-Scale Experiments

2.1 Experimental setup

Figure 3 shows the experimental setup for large-scale experiments taking place in the large wave flume (105 m (l) \times 0.8 m (w) \times 2.5 m (d)) containing a sandbed sized 600 cm in length with thickness h_s of 55 cm. The sandbed was located at the midsection of the flume whose water depth h was 34.4 and 50 cm, respectively.

Water supply pipes connected to an electric pump are installed at the bottom of the sandbed. Adjusting a flow valve between the supply pipes and electric pump changes the seepage flow rate. Figure 4 is a photo showing the array of water supply pipes installed at the sandbed bottom, being spaced with an interval P_i of 6 cm. By shutting pipe inlet valves, P_i can be adjusted to 12 or 24 cm. As indicated in the inset, the pipe inner diameter is 1.6 cm and holes with a diameter of 0.35 cm are located every 5 cm to supply water into the sandbed. Water supply pipes are covered with filter to prevent sand from clogging the water supply holes.

Two kinds of sand were used as sandbed material (Table 1). One is Niigata sand which is relatively coarse sand with grain size $D_{50} = 0.39$ mm; while the other is Soma No. 6 sand which is the fine sand with $D_{50} = 0.18$ mm. Permeability k is 0.17 and 0.042 cm/s, respectively. To clarify different liquefaction stages, we varied upward seepage flow rate, V_d , of pore water. Pore water pressure was measured at the bottom of the sandbed. To represent the hydraulic gradient due to seepage flow, equivalent hydraulic gradient H_{ge} is used, being the ratio of V_d to k .

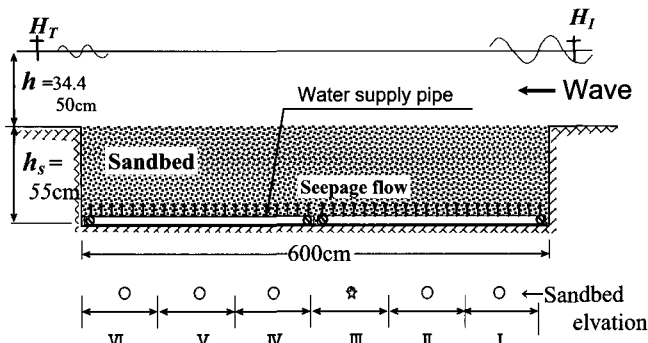


Fig. 3 Experimental setup for large-scale experiments

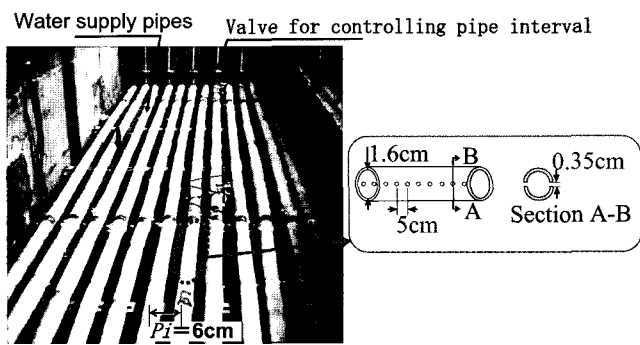


Fig. 4 Water supply pipes arrayed at the bottom of the sandbed

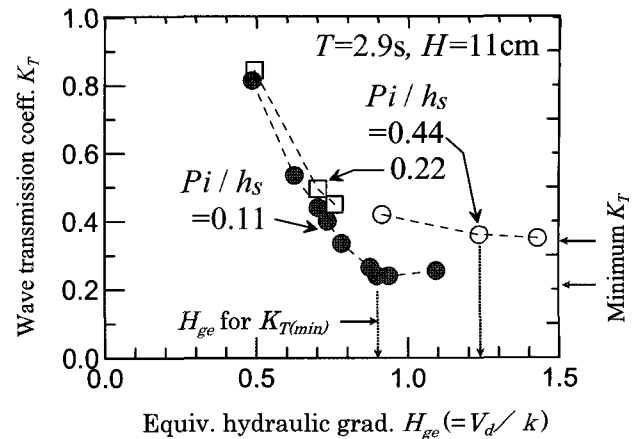
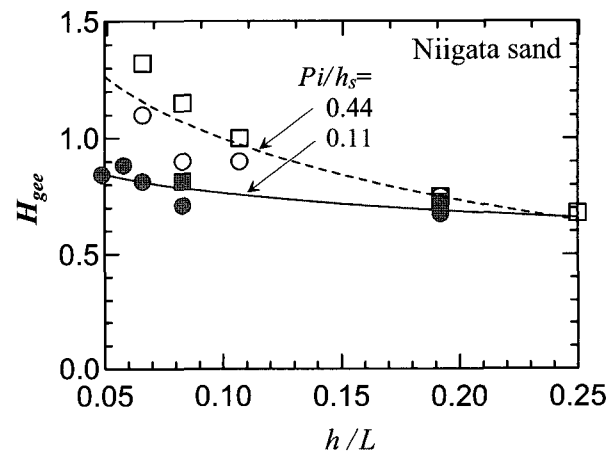
Table 1 Characteristics of sand used in the experiments

Sand name	Grain size D_{50} (mm)	Specific gravity G_s	Permeability k (cm/s)	Porosity n
Niigata	0.39	2.65	0.172	0.41-0.47
Soma No.6	0.18	2.64	0.042	0.40-0.49

We evaluated attenuation of water waves propagating along the liquefied sandbed using wave transmission coefficient K_T , which is the ratio of transmitted wave height to the incident wave height. To investigate wave-induced compaction, sandbed height is measured along the entire length at 6 points (sections I-VI, Fig. 3) separated 1 m apart. Pore water pressure at the bottom of sandbed is also measured. Optimal conditions for producing a uniform liquefied sandbed were investigated using another facility, i.e., a basic sand tank generating only upward seepage flow (with no waves).

2.2 Influence of water supply pipe interval

Figure 5 shows the wave transmission coefficient K_T versus the equivalent hydraulic gradient H_{ge} ($=V_d/k$) for Niigata sand using $P_i/h_s = 0.11, 0.22$ and 0.44 . Increases in H_{ge} cause K_T to

Fig. 5 Wave transmission coefficient K_T vs. equivalent hydraulic gradient H_{ge} for indicated values of P_i/h_s using Niigata sand with $h = 34.4$ and $h_s = 55$ cmFig. 6 Necessary equivalent hydraulic gradient H_{gee} vs. relative water depth h/L for indicated values of P_i/h_s using Niigata sand

decrease until K_T becomes constant or slightly increase. Since a smaller pipe interval produces K_T values that are comparatively lower, and low K_T values occur at relatively small H_{ge} , this indicates that reducing the pipe interval produces a more homogeneously liquefied sandbed.

Figure 6 shows variations in necessary equivalent hydraulic gradient H_{gee} versus relative water depth h/L for Niigata sand using $P_i/h_s = 0.11$ and 0.44 . In this case, H_{gee} is the minimum H_{ge} in the region of nearly constant K_T shown in Fig. 5. Note that for $P_i/h_s = 0.44$ (larger pipe interval), H_{gee} tends to increase with decreasing h/L ; whereas for $P_i/h_s = 0.11$ (smaller pipe interval) it is nearly constant over h/L . The larger H_{gee} for the larger pipe interval is caused by partial boiling due to the non-uniform distribution of seepage flow

produced in the sandbed by the water supply. Such non-uniform distribution deteriorates the efficiency of the seepage flow in forming a homogeneous liquefied sandbed.

Figure 7 shows the critical hydraulic gradient H_{gr} versus Pi/h_s for each type of sand. A basic sand tank was used to generate an upward seepage flow under no wave action. In theory, the liquefaction phenomenon occurs when the hydraulic gradient in the sandbed reaches H_{gr} defined as $(G_s-1)(1-n)$; where G_s is the specific gravity and n the porosity of the sandbed. The experimental H_{gr} is generally smaller than the theoretical value because it is obtained as a spatial average. Thus, as the difference between the theoretical and experimental value becomes smaller, the more homogeneously the sandbed is liquefied. As indicated, for both types of sand, H_{gr} tends to decrease with increasing Pi/h_s , and the difference between experimental and theoretical values is small for $Pi/h_s < 0.2$. In addition, Soma No. 6 sand shows a comparatively larger difference with increasing Pi/h_s .

Taken together, these results indicate that the small pipe interval can produce the more homogeneously liquefied sandbed and liquefy the sandbed even by much less amount of supply water. In other words, to liquefy the sandbed with high homogeneity, pipe interval Pi should be less than 20% the thickness of the sandbed for no wave action (Fig. 7); and with wave action present, it must be much smaller than 20% due to wave-induced compaction of liquefied sandbed. We accordingly consider that the water supply pipe interval

should be less than about 10% the thickness of the sandbed in order to obtain a more homogeneously liquefied sandbed. Figure 7. Variations in critical hydraulic gradient H_{gr} due to increasing pipe interval Pi/h_s (results using basic sand tank).

2.3 Wave-induced sandbed compaction

Figures 8 and 9 respectively show typical measured data for Soma No. 6 and Niigata sand for waves with a wave period of 3.3 sec at a water depth 34.4 cm. Indicated are water

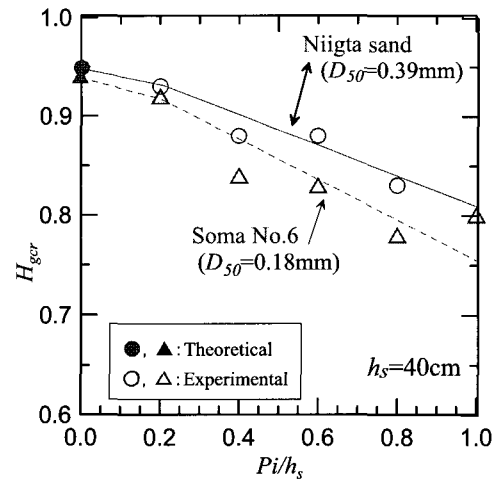


Fig. 7 Variations in critical hydraulic gradient H_{gr} due to increasing pipe interval Pi/h_s (results using basic sand tank)

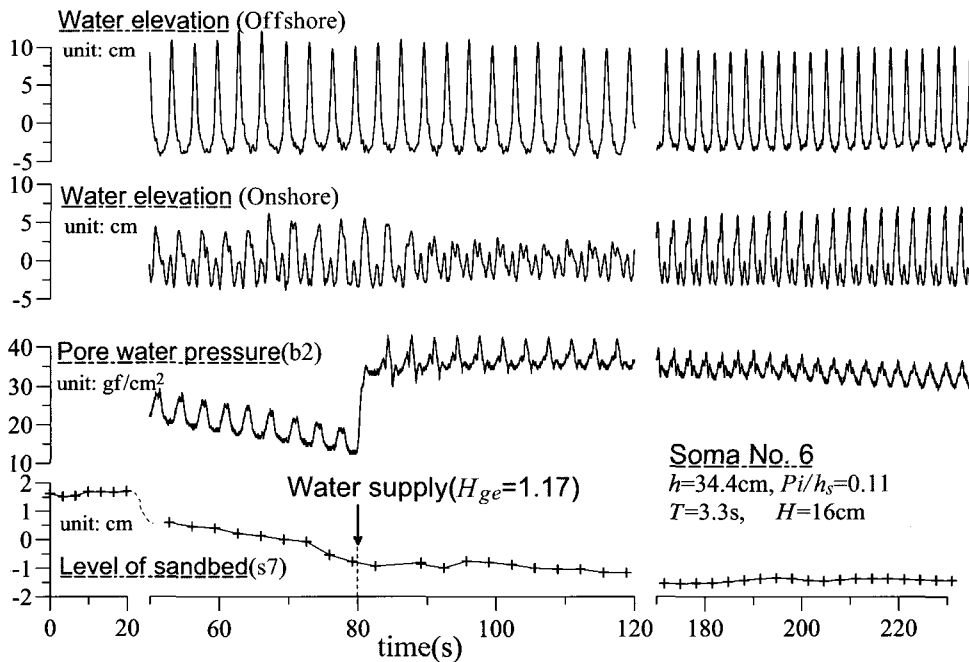


Fig. 8 Typical water elevations, pore water pressure, and mean level of sandbed measured for Soma No. 6 sand ($T = 3.3$ s, $H = 16$ cm, $h = 34.4$ cm, $h_s = 55$ cm)

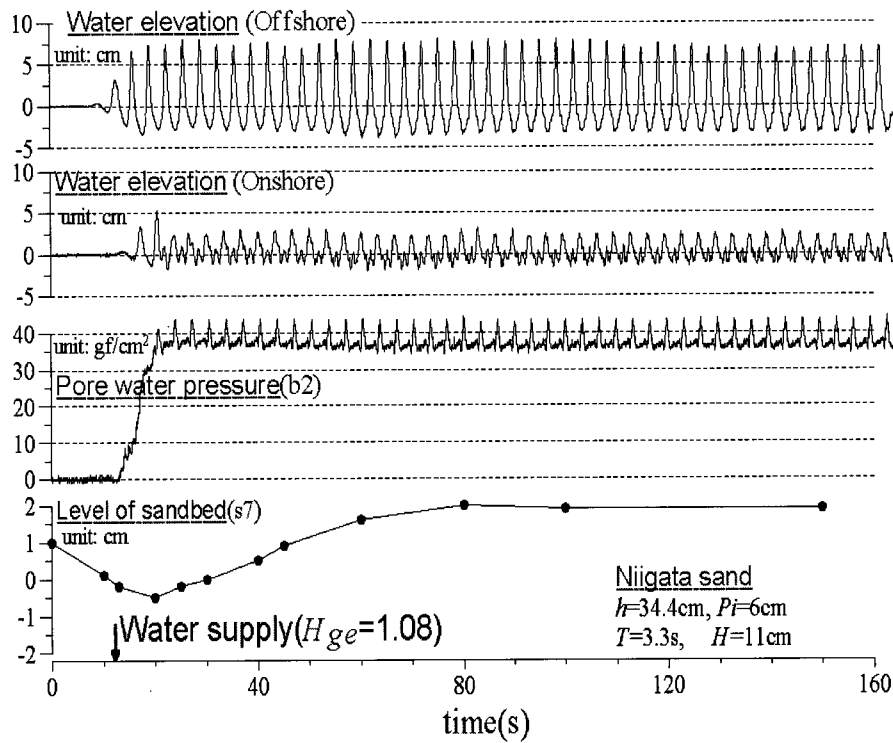


Fig. 9 Typical water elevations, pore water pressure, and mean level of sandbed measured for Niigata sand ($T = 3.3$ s, $H = 11$ cm, $h = 34.4$ cm, $h_s = 55$ cm)

elevation at the offshore and onshore side, pore water pressure at the lower layer of the sandbed, and sandbed height.

Regarding Soma No. 6 sand, after the sandbed is initially liquefied the water supply is stopped ($t = 0$ s). Note that as time increases the sandbed gradually settles, mean pore pressure decreases, and substantial wave damping is present. Then at $t = 80$ s, water supply ($H_{ge} = 1.17$) is initiated again causing pore pressure to sharply jump to 40 gf/cm^2 ($= 0.39$ kN/cm^2) and sandbed height to slightly rise until settling and becoming hard at about 100 s. Consequently, it settles largely by 5% thickness of the sandbed at 100 second after starting water supply. Amplitude of the oscillatory pore pressure gradually also decreases. The wave height decreases largely by $K_T = 0.3$ after starting the water supply, increasing again for a given H_{ge} due to this wave-induced compaction of the liquefied sandbed.

For the Niigata sand (Fig. 9), on the other hand, when no water supply is present (no upward seepage flow) small settlement due to wave action immediately occurs and then stabilizes. Also, no wave damping is observed. After initiation of flow ($H_{ge} = 1.08$), sandbed height rises gradually and its mean height by $t = 80$ s subsequently increases to 2% compared to that by $t = 0$ s. This increase in sandbed height

produces large wave damping ($K_T = 0.3$). No compaction of the sandbed occurred for Niigata sand.

From figures 8 and 9, it is noted that because the minimum K_T values for both sandbed are nearly equal each other, the grain size of the sand does not affect wave damping due to a liquefied sandbed.

Figure 10 shows the measured settlement rate of the sandbed due to wave actions for both sands, where the vertical axis indicates settlement rate R_{ssb} , which is the ratio of wave-induced settlement to the sandbed thickness h_s , and the horizontal axis the equivalent hydraulic gradient H_{ge} . At $H_{ge} = 0.4$, R_{ssb} reaches a maximum at about 0.09 for both sands, then decreases with increasing H_{ge} . This behavior indicates that increasing the supply pore pressure prevents wave-induced compaction of the liquefied sandbed.

The necessary H_{ge} values for a zero wave-induced settlement rate for the Niigata and Soma No. 6 sand are about 1.0 and 1.7, respectively. The larger value for the Soma No. 6 sand is due to more boiling, which is the result of larger seepage flow. In other words, the liquefied sandbed by seepage flow is easier to be non-homogeneous in the fine sandbed than in the coarse sandbed.

As indicated in figures 8 and 9, although wave-induced settlement for the Niigata sandbed was not observed since H_{ge}

= 1.08, substantial compaction for the Soma No.6 sand correspondingly occurred at $H_{ge} = 1.17$ which is much smaller than the necessary value of $H_{ge} = 1.7$ for the Soma No.6 sand. The large supply water, such as $H_{ge} = 1.7$, can prevent wave-induced compaction of liquefied sandbed, but it should be noted that this amount consequently leads to low wave damping.

2.4 Countermeasures against Inhomogeneity and wave-induced compaction

A successful prototype LSWB system must generate a homogeneous sandbed that is not compacted by wave actions. To do this:

- (i) the interval between water supply pipes should be less than 10% of the sandbed thickness, and
- (ii) water must be supplied uniformly through the water supply holes, regardless if the sandbed undergoes partial boiling or compaction.

To achieve (ii), it is necessary to use small holes or/and to cover the water supply pipes with a filter having lower permeability, both of which enable water to be supplied more uniformly. The filter for improving the water supply will increase flow resistance as the flow rate increases; hence the flow rate through water supply pipes is more uniform, as well as preventing sand from clogging the water supply holes as previously planned. Details on the design criteria for improving the LSWB system are contained in Kang et al. (1999).

3. Prototype Experiments

3.1 Prototype LSWB system

Based on the proposed design criteria(Kang et al., 1999), a prototype LSWB system was constructed in a very large wave flume called the "Large Hydro-Geo Channe l(Shimosako et al., 2001)", which was placed in operation in March 2000 . The main channel has a length of 184 m, width of 3.5 m, and depth of 8-12 m. A piston-type wave maker is used to generate regular/irregular waves with heights up to 3.5 m. A sandbed was installed at the midsection of the wave channel, having a length of 67 m and depth of 4 m. The sandbed material is fine white sand with 0.2 mm diameter and permeability of 0.05 cm/s, being quite similar to the Soma No. 6 sand.

Figure 11 shows a photo of the array of water supply pipes installed at the bottom of the sandbed. Water supply pipes (240 in total) are situated at an interval of 27.8 cm, about 8 % the sandbed thickness. The inner diameter is 4 cm, and holes 0.4 cm in diameter are drilled along both sides at 4 cm

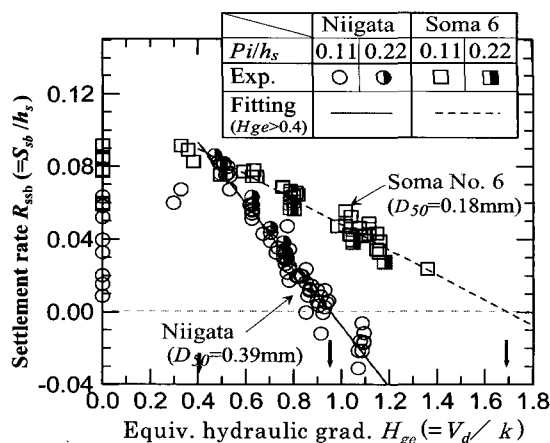
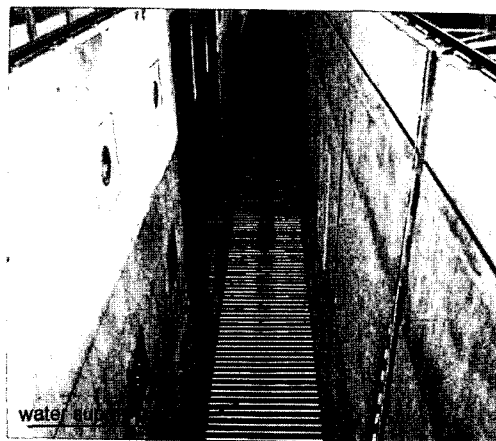
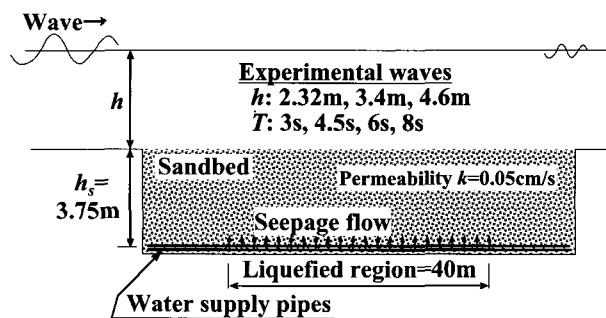


Fig. 10 Wave-induced settlement rate R_{ssb} of liquefied sandbed vs. equivalent hydraulic gradient H_{ge} for Niigata and Soma No. 6 sand ($h_s = 55$ cm)



(a) Array of water supply pipes



(b) Experimental setup

Fig. 11 Water supply pipes and experimental condition at the bottom of the Hydro-Geo Channel

intervals. Water supply pipes are covered with a low permeability filter, i.e., 0.003 cm/s at $V_a = 0.06$ cm/s. This prevents clogging and ensures uniform water flow into the

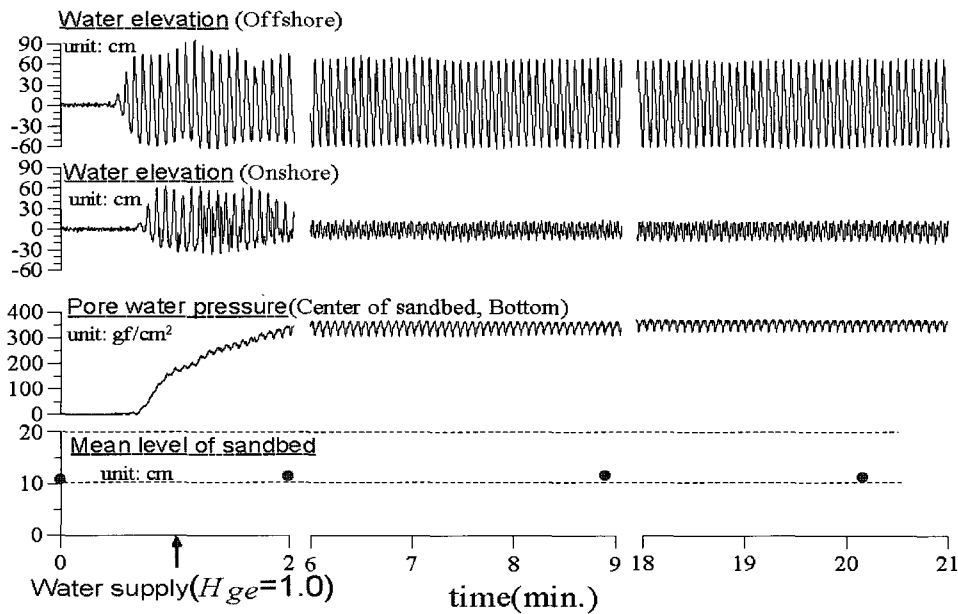


Fig. 12 Typical data of prototype experiments for the regular waves with $T = 4.5$ s, $H = 1.3$ m, and $h = 2.32$ m

sandbed.

The 40 m long, 3.75 m deep sandbed is liquefied using the seepage flow through water supply pipes constructed at the bottom of the bed. Various waves with wave periods of 3, 4.5 and 6 s were generated in water depths of 2.32, 3.4, and 4.6 m. Wave attenuation, pore pressure, and sandbed movement was measured. Since only preliminary data is discussed here, results following comprehensive analysis will be published in the future.

3.2 Preliminary analysis of experimental data

Figure 12 shows typical data for prototype experiments using regular waves with $T = 4.5$ s, $H = 1.3$ m, and $h = 2.32$ m. Data is similar to that in Figs. 8 and 9. Water flow rate corresponding to equivalent hydraulic gradient $H_{ge} = 1.0$ is supplied 1 min after wave generation, and transmitted waves are reduced in height to less than 20% that of incident waves. Despite using fine sand, there is no reduction in the wave damping effect due to wave-induced compaction. Both wave attenuation and oscillatory pore pressure are quite stable for a long time.

Figure 13 shows the effect of H_{ge} on K_T for two kinds of regular waves ($h/L = 0.083$ and 0.192) with $h/h_s = 0.625$, where the minimum K_T values are less than 0.2, being about 0.05 smaller than those obtained in the previous LSWB system (Fig. 5). Variations and minimum K_T values agree fairly well with calculations (Kang et al., 1997); and in fact, are better than compared to the results of Fig. 5. These results

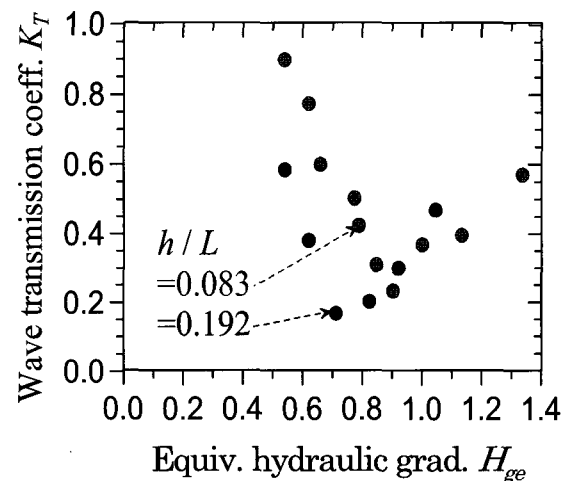


Fig. 13 Experimental results on K_T values for regular waves with $h/h_s = 0.625$

also confirm that influence of model scale on wave damping effect is negligible, thereby verifying previous results by Kang et al. (1997).

Figure 14 compares wave-induced settlement rate R_{sb} between large-scale (Fig. 9) and prototype experiments, where the settlement rate of the prototype agrees well with results using coarse Niigata sand. This clearly indicates that the improved LSWB prototype system successfully provides pore water sufficiently uniform such that wave-induced compaction does not occur despite using a fine sandbed.

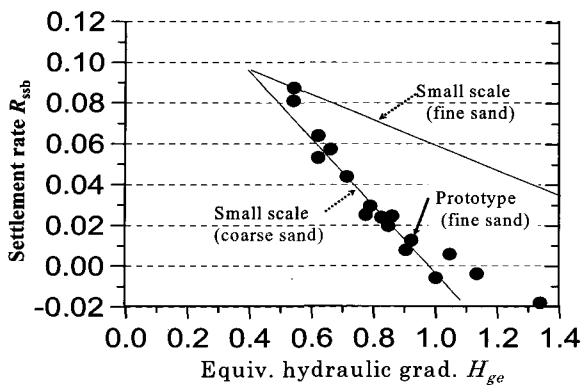


Fig. 14 Comparison of wave-induced settlement rate R_{sb} obtained from prototype and large-scale experiments

4. Conclusions

A series of large-scale experiments were conducted to investigate problems associated with the development of a practical LSB system, i.e., inhomogeneous liquefaction of the sandbed and compaction due to the cyclic wave loading. The former occurs due to partial boiling caused by inhomogeneous seepage flow in the sandbed, while the latter due to cyclic wave action on a liquefied sandbed, which reduces excess pore pressure and the wave-damping effect. Both phenomena appear predominately in a fine versus coarse sandbed. We found that using a smaller interval between the water supply pipes and covering them with a low permeable filter act together to minimize such problems.

In consideration of these findings, a prototype system was constructed and tested in a very large wave channel, with results indicating homogeneous liquefaction and no wave-induced compaction of the liquefied sandbed even though the sandbed was composed of fine sand. Preliminary analysis of experimental data also showed good agreement with theoretical calculations; hence, we conclude that wave damping provided by the prototype system is high as theoretically predicted.

The main merits of LSB are that it does not obstruct ship navigation nor seawater exchange, and it need be operated only when wave absorption is necessary. With this in mind, such a system is envisioned to be highly suitable to produce a calm sea area at a harbor entrance, or in front of an exposed ferry wharf which commonly occur at isolated island locations. Regarding required energy, it is possible that wave and/or wind energy converter systems could be used. Certainly there is promise for some successful wave barrier application to be realized, and accordingly, more research is

expected in this direction.

Acknowledgments

We thank Messrs. K. Shimosako, T. Takano, T. Kuroda, and X. Okudaira, Maritime Structure Laboratory, Port and Airport Research Institute, Japan for their valuable assistance during model experiments.

References

- Biot, M.A. (1962). "Mechanics of deformation and acoustic propagation in porous media", *J. of Applied Physics*, Vol 33, pp 1482-1498.
- Gade, H.G. (1958). "Effects of a nonrigid, impermeable bottom on plane surface waves in shallow water", *J. of Marine Research*, Vol 16, No 2, pp 61-82.
- Kang, Y.K., Takahashi, S., Suzuki, K., Miura, H. and Park, W.S. (1997). "Wave-absorbing effect of liquefied sandbed wave barrier", *Proc. of 44th Japanese Conf. on Coastal Engineering*, JSCE, pp 706-710(in Japanese).
- Kang, Y.K., Takahashi, S., Yamamoto, S., Miura, H., Takano, T., Shimosako, K. and Suzuki, K. (1999). "Development of a new wave absorbing system using a sand liquefaction", *Report, Port and Harbour Research Institute, Ministry of Transport, Japan*, Vol 39, No 3, pp 29-89(in Japanese).
- Putnam, J.A. and Johnson, J.W. (1949). "The dissipation of wave energy by bottom friction", *Trans. Amer. Geophys. Union*, 30, No 1, pp 67-74.
- Reid, R.O. and Kajiura, K. (1957). "On the damping of gravity waves over a permeable sea-bed", *Trans. Amer. Geophys. Union*, 38, pp 662-666.
- Shimosako, K., S. Takahashi, K. Suzuki and Kang, Y.K. (2001) "Large-Scale Experiments in the Large Hydro-Geo Flume", *Proc. of the International Workshop on Advanced Design of Maritime Structures in the 21st Century*, Port and Airport Research Institute, Japan, pp 28-35.
- Takahashi, S., Yamamoto, Y. and Miura, H. (1994). "Fundamental characteristics of a new wave absorbing system utilizing sand liquefaction", *Proc. 24th Int. Conf. on Coastal Engineering*, Kobe, pp 2698-2711.
- Yamamoto, T. and Takahashi, S. (1985). "Wave damping by soil motion", *ASCE, WW*, Vol 111, No 1, pp 62-77.
- Yamamoto, T., Takahashi, S. and Schuckman, B. (1983). "Physical modeling of sea-seabed interactions", *ASCE, EM*, Vol 109, No 1, pp 54-72.

2006년 7월 3일 원고 접수

2006년 8월 17일 최종 수정본 채택